# Active deformation and Plio-Pleistocene fluvial reorganization of the western Kura Fold-Thrust Belt, Georgia: implications for the evolution of the Greater Caucasus mountains and seismic hazard



| | |
|---|---|
| Journal: | *Geological Magazine* |
| Manuscript ID | GEO-19-2397 |
| Manuscript Type: | Original Article |
| Date Submitted by the Author: | 28-Nov-2019 |
| Complete List of Authors: | Sukhishvili, Lasha; Ilia State University, Institute of Earth Sciences and NSMC<br>Forte, Adam; Louisiana State University, Department of Geology & Geophysics<br>Merebashvili, Giorgi; Ilia State University, Institute of Earth Sciences and NSMC<br>Leonard, Joel; Arizona State University, School of Earth and Space Exploration<br>Whipple, Kelin; Arizona State University, School of Earth and Space Exploration<br>Javakhishvili, Zurab; Ilia State University, Institute of Earth Sciences and NSMC<br>Heimsath, Arjun; Arizona State University, School of Earth and Space Exploration<br>Godoladze, Tea; Ilia State University, Institute of Earth Sciences and NSMC |
| Keywords: | Tectonic geomorphology, Alazani basin, Gombori range, Paleocurrent analysis, Burial age dating, Greater Caucasus, Kura Fold-Thrust Belt |
| | |

# Active deformation and Plio-Pleistocene fluvial reorganization of the western Kura Fold-Thrust Belt, Georgia: implications for the evolution of the Greater Caucasus mountains and seismic hazard

Manuscript category: Tectonics and Structural Geology

Lasha Sukhishvili[1], Adam M. Forte[2], Giorgi Merebashvili[1], Joel Leonard[3], Kelin X. Whipple[3], Zurab Javakhishvili[1], Arjun Heimsath[3], Tea Godoladze[1]

[1]Institute of Earth Sciences and National Seismic Monitoring Centre, Ilia State University, Tbilisi, Georgia

[2]Department of Geology & Geophysics, Louisiana State University, Baton Rouge, LA, USA

[3]School of Earth and Space Exploration, Arizona State University, Tempe, AZ, USA

Corresponding author: Lasha Sukhishvili

Email: lasha.sukhishvili@iliauni.edu.ge

**Abstract**

Since the Plio-Pleistocene, southward migration of shortening in the eastern part of the Greater Caucasus (GC) into the Kura foreland basin has progressively formed the Kura-Fold Thrust belt (KFTB) and Alazani piggyback basin, which separates the KFTB from the GC. Previous work argued for an eastward propagation of the KFTB, implying that the western portion in Georgia is the oldest, but this hypothesis was based on coarse geologic maps and speculative ages for units within the KFTB. Here we investigate this hypothesis and focus on the Gombori Range (GR), which defines NW edge of the belt. Previous work divided the sediments of northern flank of the range into three facies. The rock types in the older and middle facies suggest a GC source provenance, despite the modern drainage network in the NE GR, which is dominated by NE flowing rivers.

Paleocurrent analyses of the alluvial conglomerates of the oldest and youngest syntectonic units indicate a switch from dominantly SW directed paleocurrents in the oldest unit to paleocurrents more similar to the modern drainage network in the youngest unit. A single successful 26Al-10Be burial date indicates these syntectonic sediments are 1±1 Ma, which while not a precise age, is consistent with original mapping suggesting these sediments are Akchagyl-Apsheron (2.7-0.88 Ma) age. Tectonic geomorphologic analyses indicate that western GR is the most active. Given its close proximity to the capital city of Tbilisi, this suggests that active structures within the Gombori range pose seismic hazard to this city of 1.2 million people.

## 1. Introduction and Motivation

The Kura Fold-Thrust belt (KFTB) is located between the Greater Caucasus (GC) and Lesser Caucasus Mountains and represents a major structural system within this region, accommodating shortening between these two orogenic systems (e.g. Forte *et al*. 2010; Forte *et al*. 2013). Closure of the Greater Caucasus back-arc basin in the late Miocene and the transition from subduction to collision in the Pliocene, resulted in a fast exhumation phase of the Greater Caucasus (Avdeev & Niemi 2011), however the exact timing of collision along-strike remains controversial (e.g. Cowgill *et al*. 2016; Vincent *et al*. 2016). Since the Plio-Pleistocene, much of the shortening in the eastern half of the Greater Caucasus has propagated southward, into the Kura foreland basin, and formed the KFTB (**Error! Reference source not found.**). Since initiation of deformation within the KFTB, it has accommodated approximately half of total Arabia-Eurasia convergence at the longitude of the eastern GC (Forte *et al*. 2013). Geodetic measurements indicate that there is an along-strike, eastward increasing velocity gradient between the Greater and Lesser Caucasus, with approximately 8 mm/yr of expected convergence between the two ranges at the longitude of the center of the KFTB (Reilinger *et al*. 2006). However, while efforts are ongoing to densify the GPS network throughout the KFTB, at present station coverage is not sufficient to perform further analyses. By analyzing large twentieth century earthquakes in eastern Turkey and the Caucasus and expected Arabia-Eurasia motion, Jackson & Mckenzie (1988) and Jackson (1992) hypothesized that the Caucasus must be deforming mostly aseismically, either by creep on faults or by folding. It might be expected that shortening, especially by folding, of thick, possibly overpressurized, sediments, should occur without generating major earthquakes, even if folding were to occur above buried

(blind) thrust or reverse faults (Jackson, 1992). Nevertheless, from the eastern domain of the KFTB in Azerbaijan, there are strong indications that the Kura fold-thrust belt is actively deforming (Forte *et al*. 2010 and 2013; Mosar *et al*. 2010) and thus the potential seismic hazard within the fold-thrust belt may be underestimated. There are several Mw 5-5.4 earthquakes within the KFTB area in the Complete Catalogue of Instrumental Seismicity for Georgia (Onur, *et al.* 2019). The earthquake data indicates a south-dipping low-angle thrust under the Gombori ridge, which is consistent with geologic observations throughout the KFTB (Forte *et al*. 2010, 2013; Adamia *et al*. 2010, 2011) The strike of the fault plane of a M 5.4 event (27.11.1997) was approximately east-west (Tan & Taymaz, 2006), also consistent with the structural geometries within the KFTB (Figure 2). However, detailed paleoseismic studies have never been conducted in the region, leaving significant uncertainties about the seismic hazard.

Previous work on the KFTB noted that there is more elevated topography (measured with respect to the adjacent basins), cross-strike width, and older structures exposed in the western part of the belt. Forte *et al.* (2010) argued this pattern could be caused by an eastward decrease of total shortening, timing of initiation, or combination thereof. According to *Alania et al. (2017)*, the formation of Kakheti Ridge (located at the western part of KFTB, here referred to as the Gombori Range), took place in the Pliocene, while estimates of the initiation of deformation within the eastern segment of the belt lie between 1.8-1.5 Ma by Forte *et al.* (2013), though more recent dating of Eastern KFTB stratigraphy suggests deformation may have initiated closer to 2.2-2.0 Ma (e.g. Lazarev *et al.* 2019). This is consistent with the idea first proposed by Forte et al. (2010) that deformation started in the western KFTB and propagated eastward. While these independent studies show a consistent eastward propagating pattern of

deformation and deformation initiation age along-strike within the KFTB, this is complicated by the fact that there is a better understanding of stratigraphy and the deformation pattern of the central and eastern part of KFTB, whereas much remains uncertain about the western domain.

Additional evidence of along-strike variation in structural history is interpretable from the topography and comparisons between the modern drainage network and the paleo-drainage network of the KFTB as reconstructed from alluvial stratigraphy. Specifically, in the eastern KFTB, south flowing rivers sourced from the GC still cross the KFTB, but west of where the Alazani river enters the KFTB, no south flowing river from the GC crosses the KFTB (Figure 1). It is a reasonable expectation that prior to the development of the KFTB and during some portion of the deposition of pre and syntectonic alluvial sediments now exposed within the KFTB, some GC-sourced rivers did make it to, or through, the KFTB. Such drainage reorganizations during the progressive growth of fold belts is observed in both natural examples (e.g. Bretis *et al.* 2011; *Burbank et al.* 1996; Davis *et al.* 2005; Delcaillau *et al.* 1998; Delcaillau *et al.* 2001; Delcaillau *et al.* 2006; Keller *et al.* 1999; Lawton *et al.* 1994) and experiments (e.g. Champel *et al.* 2002; (Douglass and Schmeeckle 2007). The timing of drainage reorganization in the western KFTB would provide an important constraint on the structural and topographic evolution of this portion of the KFTB and thus help constrain the along-strike evolution of the KFTB overall.

To investigate how compatible the geology of the western segment of the KFTB is to the above proposed models, we applied quantitative tectonic geomorphologic approaches, $^{26}$Al-$^{10}$Be burial dating, and paleocurrent analyses within the Gombori Range.

## 2. Stratigraphic background

The Gombori range, which is the highest relief part of the KFTB and defines the NW edge of the belt, is built by deformed lower and upper Cretaceous, Eocene and Oligocene, Miocene, Plio-Pleistocene and Quaternary period rocks (Figure 3. *Stratigraphy of the Gombori range compiled after (Buleishvili, 1974), (Zedginidze* et al. *1971), (Kereselidze, 1950), (Sidorenko & Gamkrelidze, 1964), (Buachidze* et al. *1950)*. Here we focus exclusively on the Plio-Pleistocene sediments of the Gombori range.

Previous work has described the Plio-Pleistocene sediments of the Gombori range as a part of the Akchagyl-Apsheron regional stages and are collectively described as the Alazani series. Within the Caspian Sea region and its subbasins, the Akchagylian regional stage corresponds to the late Pliocene epoch (Jones & Simmons, 1996; Krijgsman *et al.* 2018). The Akchagylian represents a series of large transgressions, which temporarily re-established marine connections between Caspian Sea and world ocean (Jones & Simmons 1996; Forte & Cowgill, 2013; Van Baak *et al.* 2019). The Akchagylian sediments are broadly considered as being deposited in a marine environment (Jones & Simmons 1996), but there are continental facieses of Akchagylian stage within the eastern (Forte *et al.* 2015) central and western KFTB as well (Chkhikvadze *et al.* 2000; Alania *et al.* 2017; Sidorenko & Gamkrelidze, 1964). The Apsheronian stage, which overlies the Akchagylian, is essentially regressive in character and corresponds to lower and middle Pleistocene (Jones & Simmons, 1996; Krijgsman *et al.* 2018). It generally represents shallow marine and continental deposits, but within the Gombori range, Apsheronian sediments are considered part of the Alazani series, which has previously been interpreted as being deposited in a terrestrial environment (Sidorenko & Gamkrelidze, 1964).

The maximum thickness of the Alazani series at the NE slope of Gombori range is ca. 1800m (Sidorenko & Gamkrelidze, 1964) between catchments 7 (riv. Kisiskhevi) and 12 (riv. Papriskhevi) (Figure 3) (Buachidze *et al.* 1950; Buleishvili, 1974) and thins to ca. 1400m along the SW slope of the Gombori range (Sidorenko & Gamkrelidze, 1964).

Three facies, $Al_1$, $Al_2$, and $Al_3$ have been previously defined within the Alazani series. There is an angular unconformity at the base of the Alazani series between it and the older Neogene, Paleogene and Cretaceous sediments. Angular unconformities are also present between all of the Alazani series facies.

The lower $Al_1$ is represented by well-consolidated conglomerates and cobbles with 0.2-1.5m thick lenses of loams and clays. The lowest boundary of the $Al_1$ facies is marked by a bluish color conglomerate (Figure 4). The longest axis of cobbles within this conglomeratic interval averages between 10-15cm. Sandstone, schist, limestone and marl clasts are the dominant rock types of cobbles and conglomerates within the $Al_1$ facies. Some of these rock types here (e.g. schists) are typical for the Greater Caucasus and suggest that these sediments are sourced broadly from the north (Buachidze *et al.* 1950; Sidorenko & Gamkrelidze, 1964), but detailed provenance analyses of these sediments are yet to be performed. The thickness of the $Al_1$ facies is ca. 700m. The $Al_1$ layers broadly define the Gombori range as an anticlinorium, with $Al_1$ layers dominantly north dipping at ca. $50\text{-}60^0$ along the NE slope and southeast dipping at ca. $20\text{-}45^0$ along the southern slope. Surface elevation of exposures of the lower boundary of $Al_1$ facies within Gombori range is at 481m, but as it is challenging to distinguish between the lower $Al_1$ and upper $Al_3$ facies in the field, and thus a clear upper limit for $Al_1$ facies are not estimated yet, but it might reach to 1991m.

The overlying $Al_2$ facies is mostly dominated by loam and clay, but small amounts of cobbles and conglomerates are also present. As in the $Al_1$ facies, the rock types in this facies are also suggestive of a Greater Caucasus source (Buachidze *et al.* 1952). The maximum thickness of this facies is ca. 500m at catchment 6 and gradually decreases to 50m to South-Eastern direction (Buachidze *et al.* 1952). In the northern slope of the Gombori, the $Al_2$ facies dip to the NE, but at shallower angles with respect to the underlying $Al_1$ facies, with average dips in $Al_2$ facies rocks being ca. $20^0$-$30^0$. This facies contains a thin layer of volcanic ash (Figure 5). The surface elevation of $Al_2$ facies exposures within Gombori range varies between 448 and 1569m.

The upper $Al_3$ facies is dominantly composed of conglomerates with minor interbeds of loams and clays. According to some reports (e.g. Kereselidze, 1950) another volcanic ash layer of 0.4 m thickness is traceable within loamy layer of catchments 6 and 7, but we did not observe this ash layer in the field. The thickness of this facies is between 150-250m. Layers within the $Al_3$ facies exposed along the NE edge of the Gombori dip shallowly to the NE at $5$-$15^0$. The surface elevation of exposures of $Al_3$ facies within the Gombori range varies between 390 – 1210m. There also exist isolated packages of conglomerate higher in the Gombori range that are unconformable with the underlying, older stratigraphy, and are likely exposures of the Alazani series. These exposures may be associated with the $Al_3$ facies, but could also be associated with the $Al_1$ facies as outside of their stratigraphic context, it is difficult to distinguish between these two facies.

## 3. Methods

### 3.a. Paleocurrent analyses

Modern rivers draining the NE slopes of the Gombori range flow NE and drain into the Alazani valley, but archival data of geological reports (Buachidze *et al.* 1950; Buachidze *et al.* 1952) suggests that the alluvial sediments of the Alazani series contain rock types typical for the Greater Caucasus, suggesting a southward flow of rivers during the deposition of at least some of the sediments.

Alluvial channels are very sensitive to active tectonics and adjust to vertical deformation or base level change by channel modification (Merritts *et al.* 1994). Research on fluvial terraces (as abandoned floodplains) using gravel or pebble imbrication, is one of the reliable indicators of paleocurrent in coarse grained deposits and can shed light on tectonic evolution of the site (Miao *et al.* 2008). The direction of imbrication of oblate clasts in a conglomerate can be used to indicate the direction of the flow that deposited the gravel (Nichols, 2009).

Exposures of Alazani series sediments in the walls of canyons along the main stem rivers of catchments 7 and 11 were selected for paleocurrent analyses. A total of 265 clasts were measured from four sites of $Al_1$ and $Al_3$ facies of both catchments. In this study, we measured the orientation of the clast imbrication with a Brunton compass and performed unfolding and further processing using Stereonet 10 software (Allmendinger *et al.* 2011). We performed this paleocurrent analysis to specifically test whether there was evidence of flow reversal and/or drainage reorganization during the deposition of the potentially syntectonic Alazani series sediments.

**3.b. Tectonic geomorphology**

Topography reflects the balance between rock uplift, driven by tectonics, and erosional and depositional processes modulated by climate and lithology. With careful consideration of potential climatic and lithological complications, quantitative geomorphic analyses can constrain relative differences in rates of rock uplift, and thus inform our understanding of tectonics (e.g., Kirby & Whipple, 2001; Wobus *et al.* 2006; Dibiase *et al.* 2010; Kirby & Whipple 2012; Whittaker, 2012; Whittaker & Boulton 2012; Rossi *et al.* 2017; Gallen & Wegmann 2017). Importantly, in the absence of other data, e.g. dense geodetic networks and/or long-term and complete seismic and paleoseismic records, tectonic geomorphology can also be useful in highlighting areas of active tectonics and potential seismic hazard (e.g. Kirby *et al.* 2008).

To evaluate the activity within the western end of the KFTB, we selected the twelve largest catchments (14-108 $km^2$) along the northern slope of Gombori range and calculated several morphometric parameters using TAK (Forte & Whipple, 2018), TopoToolbox (Schwanghart & Scherler, 2014), and QGIS using a digital elevation model (DEM) acquired through the ALOS AW3D30. The DEM is produced by the Japan Aerospace Exploration Agency (JAXA) and has a horizontal resolution of ~30m (available from http://www.eorc. jaxa.jp/ALOS/en/aw3d30/index.htm). The AW3D30 DEM dataset was generated based on the 0.15-arcsec AW3D DEM dataset. Two resampling methods were applied to obtain one pixel value on AW3D30 from 7 by 7 pixels on AW3D. The first one is used the averaging method (Ave), which is simply calculated as an average value from appropriate 49 pixels except for masked out values. Another is the medium method (Med), which is selected a medium height value i.e. 25th height from 49 pixels. If it shows a masked value, same value is kept in AW3D30.

The both Ave and Med datasets are contained in individual AW3D30 dataset, which can be downloaded free of charge. AW3D30 Ave DEM has vertical accuracy of 5 m (RMSE) (Tadono *et al.* 2016) using the EGM96 vertical reference frame (JAXA 2017). In this study, the average dataset is used.

We attempted to limit our analyses to areas that were bedrock streams, as many of the metrics were designed for application to bedrock rivers. Thus, we avoid the lower portions of catchments as these portions of the rivers are likely more alluvial in character and, additionally, are zones of intense agricultural activities and other human modifications.

Another important point is the relationship between climate, i.e. precipitation, and tectonics and how this relationship is reflected in the topography of actively deforming regions, which is a long-standing debate (e.g. Whipple, 2009). We generally expect that topography may reflect spatial variations in precipitation, so it is important to characterize precipitation as part of a topographic analysis (e.g. Kirby & Whipple, 2012).

We use satellite data from the Tropical Rainfall Measurement Mission (TRMM) 3B42 V7 collected from 1998–2017. TRMM dataset contains daily rainfall information recorded in 30km size pixels. TRMM derived rainfall data is well-tested in tectonic geomorphologic studies in Caucasus (Forte *et al.* 2016), Andes (Bookhagen & Strecker, 2008) and Himalayas (Bookhagen & Burbank, 2006). **Error! Reference source not found.** shows that all twelve catchments are covered by five TRMM pixels.

Similar to climatic influences on topography, lithology and contacts between very different lithologies can produce patterns in topography that may be confused with tectonic signals (e.g.

Mitchell & Yanites, 2019). Different lithological units can have different resistances to erosion, which can be a strong control on channel gradient and topography. Lithological contacts and catchment-dominant rock types were identified to include in tectonic geomorphologic analyses. To check the correlations between lithological units (including rock properties) and topographic indices we compiled several geological Soviet era geologic maps with new field observations and mapping. For each catchment, we calculated dominant rock types (according to surface area) to correlate this data to other tectonic geomorphologic proxies.

For our quantitative topographic analyses, we calculated the normalized channel steepness index ($K_{sn}$), catchment-averaged normalized channel steepness index, total catchment relief, catchment-averaged hillslope gradient ($S_{avg}$), catchment-averaged local relief calculated using a 1km-radius circle, and drainage area for all selected catchments.



**3.b.1. Channel steepness index**

Normalized channel steepness index is an important topographic metric in active ranges (e.g. Dibiase *et al.* 2010). Despite incomplete understanding of the varied processes contributing to fluvial erosion, the stream profile method has proven an invaluable qualitative tool for neotectonic investigations. When controlling for differences in precipitation and lithology, empirical observations and simple models of fluvial erosion suggest a positive correlation between channel gradient and rock uplift rate (e.g. Wobus *et al.* 2006).

Typical river longitudinal profiles, for both bedrock and alluvial rivers, are concave and can be described by an empirical power law relationship between slope and area:

$$S = k_{sn} A^{-\theta}, \text{ and}$$

$$k_{sn} = \frac{S}{A^{-\theta}}$$

where S is slope, $K_{sn}$ is the normalized channel steepness index, A is the upstream contributing drainage area, and θ is the channel concavity index (Flint, 1974) Numerous studies indicate that the most channels have uniform concavity regardless of the uplift rate (Snyder *et al.* 2000; Whipple, 2004), because the concavity index (θ) is relatively insensitive to differences in rock uplift rate, climate or substrate lithology at steady-state (provided such differences are uniform along the length of the channel), while the steepness index ($k_s$) varies with these factors, therefore steepness index is a useful metric for tectonic geomorphic studies (Kirby & Whipple, 2012).

To normalize channel steepness indexes, we used a reference concavity ($\theta_{ref}$) of 0.5, because in practice, it is found that values of $\theta_{ref}$ between 0.4 and 0.5 work well for most mountain rivers (Kirby & Whipple, 2012). Normalization of the channel steepness index allows for the comparison of river profile morphology between streams and watersheds of different drainage areas.

**3.b.2. Catchment-averaged local relief**

Local relief is the difference between minimum and maximum elevations within a specified distance and is strongly correlated with erosion rate (Ahnert, 1970; Montgomery & Brandon,

2002; Kirby *et al.* 2003; Dibiase *et al.* 2010), which is well-correlated to rock uplift rate (e.g. Kirby & Whipple, 2001; Lague, 2014) We used 1km radius circle to generate local relief.

**3.c. Cosmogenic nuclide burial age dating**

The ages of the Alazani series sediments are particularly important as the age of these syntectonic sediments could help constrain the age of initiation of this portion of the KFTB. Because the Alazani series sediments lack abundant ash horizons and are mostly too coarse grained for magnetostratigraphy or the preservation of microfauna useful for biostratigraphic correlation, we attempted to constrain the age of these sediments through the use of cosmogenic nuclide burial age dating. Terrestrial cosmogenic nuclides (TCNs), such as $^{10}$Be and $^{26}$Al, are produced by the interaction of secondary particles, produced in the Earth's atmosphere during interaction with cosmic rays, with Earth materials (e.g. see review by Gosse & Philips, 2001). The accumulation of TCN in Earth materials is a function of depth, the duration of exposure, the erosion rate of the surface, and the production rate of the isotope in question, which is a function of latitude and elevation. Importantly, production of TCNs goes to zero below an attenuation depth such that virtually all production occurs in the first 1-3 meters of the Earth's surface. Measuring the cosmogenic nuclide abundances in sediment eroded from upland catchments and then deposited in adjacent basins records both a paleo erosion rate and a time since burial (e.g. Granger *et al.* 1997; Granger & Muzikar, 2001; Granger, 2006). As there are two unknowns, it is necessary to measure the concentration of two separate TCNs with different half lives, which in this study are $^{10}$Be and $^{26}$Al. It is assumed that both burial of these sediments and shielding from any further production of TCN post-burial (i.e. burial below

several meters) occurs rapidly and that the sediments in question remain shielded until nearly the time of collection (e.g. see review by Granger, 1997).

### 3.c.1. Sample collection and preparation

Three samples were collected for cosmogenic nuclide burial age dating – GOMSS01, GOMSS02 and GOMSS03 (see **Error! Reference source not found.**.

*GOMSS01*

The site is located in the Gombori range, 1.5 km southeast from the highest peak of the range called Tsivi (1991m). The sample was collected from the bottom of 1.0m deep pit. The upper 0.2 of this pit was soil and the rest was conglomerate of probably $Al_1$.

*GOMSS02*

The sample was taken from the lowest edge of an outcrop exposed along the Turdo river (catchment 6) from probably $Al_3$. The sampling spot was already carved out by erosion for about 1.5 – 2.0 meters, additionally we excavated back an additional 0.4 meters. Sample GOMSS02 was taken from 0.5m above the floodplain and 14m below the surface of the canyon wall. Horizontal dug depth: 0.4m, dip: $5^0$, dip direction: $2^0$.

*GOMSS03*

The sample was taken 500m upstream from GOMSS02 within the same outcrop belt along the Turdo River, from 1.88m above the floodplain from probably $Al_3$. The outcrop was horizontally carved by recent erosion inward ~0.9m and we excavated an additional 0.4m into the vertical

face. The sampling location was 66m below the surface of the canyon wall. Dip: $10^0$, dip direction: $5^0$, depth from the top of the outcrop: 66m.

*Table 1: Burial age sampling site information*

Of the three samples collected, two (GOMSS01 and GOMSS03) yielded sufficient quartz for dating. The isolation and purification of quartz, dissolution, column chemistry, and precipitation of Be and Al oxides was performed in the cosmogenic isotope laboratory at Arizona State University. Isolation of quartz in these samples required modification of standard methods (e.g. Kohl & Nishiizumi, 1992), because of significant fractions of fine-grained, quartz rich lithic material that dissolved at similar rates in HF and $HNO_3$ leaches as the quartz being targeted for analysis. Thus, after the initial step of cleaning in Aqua Regia, instead of proceeding directly to leaching in HF and $HNO_3$, we first used the hot phosphoric acid method (Mifsud *et al.* 2013) to remove feldspars and break up these lithic clasts. After HPA, samples were leached with HF and $HNO_3$ as in the standard procedure. After cleaning and during dissolution, samples were spiked with commercial $^{10}$Be carrier. We then extracted $^{10}$Be and $^{26}$Al through column chromatography (Ditchburn & Whitehead, 1994) and nuclide ratios were measured via accelerator mass spectrometry at the Purdue Rare Isotope (PRIME) Laboratory at Purdue University. We measured native Al concentrations for the two samples using a Thermo iCAP6300 ICP-OES at Arizona State University's Goldwater Environmental Laboratory.

### 3.c.2. Modeling burial age dates

For the two burial age samples that yielded sufficient quartz, we used CosmoCalc v3.0, a Microsoft Excel add-in for cosmogenic nuclide calculations (Vermeesch, 2007). We used the default settings for calibration sites for $^{10}$Be and $^{26}$Al production and production mechanisms within CosmoCalc v3.0 and report the results of using the Burial-Exposure function within CosmoCalc's Age/Erosion rate calculator, though we also tested the Burial-Erosion function, which produced similar estimations of burial age. CosmoCalc provides two different numerical methods for fitting burial dates, the Metropolis and Newton's method. We tested both methods and found that the Metropolis method, which is more complicated, produced variable burial ages, i.e. running the calculation multiple times yielded different results, but that given the magnitude of the uncertainty, this variability in burial ages was small and the error ranges for the simpler Newton's method were extremely large. Importantly, for most runs, the reported burial age using Newton's and the Metropolis method were similar and the error ranges reported from the Metropolis method were largely consistent between runs. We elected to report values from the Metropolis method as these likely reflect a more reasonable range of uncertainties on the burial ages (e.g. Vermeesch, 2007). To account for the variability in reported burial age from multiple runs of the Metropolis method, we report the average of the result of ten runs.

To determine a burial age, a production scaling factor must be assumed for the area that originally contributed the sediment that was eventually eroded, transported, deposited and then buried. While the exact parameters included in different scaling schemes vary, in general latitude and elevation will be the most important factors controlling the production rate (e.g.

Gosse & Philips, 2001). Because the source of sediment for the Alazani series sediments is not well constrained, we tested four different scaling schemes assuming different source areas. Specifically, we tested a 'local' sourcing using a latitude and mean elevation appropriate for a representative catchment in the northern Gombori range, and then three different sources from the GC with representative latitudes and mean elevations for a river draining the higher portions of the central GC (e.g. the modern Aragvi river), one draining an intermediate set of elevations (e.g. the modern Iori river), and one draining lower elevations coming directly from the small catchments that drain into the Alazani valley from the central and eastern GC. For calculation of scaling factors, we use the CosmoCalc implementation of the Desilets *et al.* (2006) scheme. The calculated burial ages are reported in **Error! Reference source not found.** for GOMSS03, calculations were not performed for GOMSS01 as an age is not interpretable for this sample as it plots in the region above the constant exposure line, outside the range of physically possible results.



## 4. Results

### 4.a. Paleocurrent analyses

Paleocurrent analyses of outcrops of $Al_1$ in two catchments indicate that $Al_1$ sediments were deposited by a river flowing in a SW direction through the modern Gombori Range, counter to the modern drainage direction and consistent with rivers sourced from the Greater Caucasus. The same analyses in the younger, stratigraphically higher $Al_3$, paleocurrents no longer indicate a single, dominant flow direction but are generally consistent with dominantly southward or eastward flow (see Figure 7 and

Table *2. Von Mises distribution results for the paleocurrent measurements*



**4.b. Tectonic geomorphology**

Quantitative tectonic geomorphologic analyzes show higher channel steepness indexes from the western catchments. Catchment-averaged local relief is also higher in the western catchments (Figure 8), which is consistent with the observation in many landscapes that mean normalized channel steepness and local relief are often linearly related (Dibiase *et al.* 2010). A simple interpretation of these two indices would suggest that the western part of Gombori range is uplifting faster than its eastern segment.

As noted above, tectonic geomorphologic proxies could be influenced by rainfall and lithology. Indeed there are strong correlations between rainfall and each of catchment-mean elevation, local relief and mean $K_{sn}$ ($r^2$=0.84, $r^2$=0.68 and $r^2$=0.89, respectively) This likely reflects expected orographic enhancement of rainfall such that areas of high relief, channel steepness and mean elevation driven by high rock-uplift rates are associated with high rates of precipitation. Importantly, a climatic control on topography would imply reduced relief and channel

steepness in areas of enhanced precipitation. Thus, interpreting topography as reflecting rock uplift rate patterns alone is a conservative assumption. We also checked whether lithology importantly influenced our tectonic geomorphologic indexes, but correlations between dominant rock types and geomorphologic proxies are low (Figure 9), as the correlation coefficients between mean $K_{sn}$ and K (Cretaceous rocks) and Ak-Ap (Akchagyl-Apsheron sediments) are 0.42 and -0.46. Higher slopes of conglomerate dominated catchments could be explained by the tendency of the conglomerate deposits to be exposed as cliffs.

The correlation matrix in Figure 9 shows very high correlation between mean $K_{sn}$ and elevation (0.95), implying faster uplift rates in the center of the Gombori range, an assumption generally consistent with the deeper levels of exposure in the center of the range, i.e. Cretaceous rocks (Figure 7 & Figure 10).

**4.c. Burial age dates**

**Error! Reference source not found.** summarizes the analytical results. Unfortunately, one of our samples, GOMSS01, yielded a $^{26}Al/^{10}Be$ ratio that even within the uncertainty bounds plots entirely above the constant exposure line of the standard erosion island plot, in the so-called 'forbidden zone' (Figure 11). Data that plots in this region is physically impossible as the $^{26}Al/^{10}Be$ ratio cannot exceed the ratio of the production rates of the two isotopes because $^{26}Al$ decays faster than $^{10}Be$. This suggests that there was a methodological error during processing, thus a burial age is not interpretable from this sample. The other sample, GOMSS03, did yield an interpretable age, but because of relatively high concentrations of native Al and low concentrations of $^{26}Al$, the analytical precision of this measurement is quite low, yielding a burial age of ~1.0 Ma, with lower and upper bounds of 0.005 Ma and 2.5 Ma, respectively (see

**Error! Reference source not found.** for complete results). While imprecise, given that there are no published geochronologic ages for the age of the Alazani series, or more broadly for any of the sediments in this region of the KFTB, this age is still meaningful as it confirms that these sediments are most likely Apsheronian in age. Because of the relatively low $^{10}$Be concentration and thus the relatively high implied paleo-erosion rates, the uncertainty in source area for the sediment and associated uncertainty in applicable production scheme does not significantly influence the interpreted age for sample GOMSS03, but does have implications for the implied paleo erosion rate (Figure 11). The minimum and maximum scaling for sample GOMSS03 would imply paleo erosion rates within the source area of between ~20 cm/ka to ~35cm/ka, respectively.



## 5. Discussion

### 5.a. Initiation and development of the western Kura Fold Thrust Belt

The results of our paleocurrent analyses suggest that a major drainage reorganization and flow reversal of rivers within the western KFTB started during or after the deposition of the $Al_1$ facies within the Alazani Series and finished during or after deposition of the $Al_3$ facies. We attribute this drainage reorganization to formation, or intensification of uplift, of the western KFTB at this longitude during the time period spanning the deposition of the Alazani Series (Figure 12).

Our field measurements show that $Al_1$ facies have higher dip angles ($50^0$-$60^0$), $Al_2$ has moderate – $20^0$-$30^0$ dip angles, and the youngest $Al_3$ facies have the shallowest dips – $5^0$-$15^0$ (e.g. Figure 7), broadly suggestive that these strata are syn-tectonic, i.e. they are growth strata. The

sediments of the Alazani series were previously mapped as being a part of the Akchagyl-Apheron stages. The reported age for the base of the Akchagyl is variable between publications and regions (e.g. Krijgsman *et al.* 2019), but it has been constrained to be ~2.7 Ma near the Azerbaijan Caspian Sea coast based on $^{40}Ar/^{39}Ar$ dating of an ash horizon (Van Baak *et al*. 2019b). It is suggested that the base of the Akchagyl may be time transgressive and in a section ~150 km to the east of the Gombori range it has been constrained to be ~2.5 Ma based on the maximum depositional age from detrital zircons in the strata below the Akchagyl (Forte *et al.* 2015). The boundary between the Akchagyl and Apsheron stages are similarly variable, but in the vicinity of the KFTB, the Apsheron has been dated to extend from 2.2 to 0.88 Ma (e.g. Krijgsman *et al.* 2019).

According to this information, we make an attempt to estimate the ages and reconstruct the depositional environment and tectonic context of the Alazani series. Deposition of $Al_1$ sediments started not earlier than ca. 2.7-2.5 Ma years ago by the streams flowing from the GC to the southwest through the location of the modern Gombori range area into the Kura basin. We hypothesize that during deposition of $Al_1$, uplift of the Gombori range initiated, and potentially damming the formerly south flowing rivers, which could explain the finer, more lacustrine sediments in $Al_2$, though given the uncertainty in the exact age of the $Al_2$ facies and the broad context of the Akchagyl stage as a transgressive event, it is not possible to rule out a more regional explanation for the lacustrine character of the $Al_2$ facies. Regardless, by the time of deposition of $Al_3$, sufficient deformation and uplift had accrued in the Gombori range to effect a significant drainage reorganization and the development of (1) a set of north flowing rivers on the Gombori range and (2) an axial valley, i.e. the Alazani valley, between the Gombori

and the GC. We interpret the lack of a dominant paleocurrent direction in these $Al_3$ facies sediments to reflect possible deposition within this axial valley, which today is dominated by a set of meandering fluvial systems. This would imply that the northwestern extent of the Gombori range has expanded since the deposition of $Al_3$, i.e. at the time of deposition the paleocurrent sites were not within the deformed part of the Gombori range, but have subsequently be incorporated into the range. Comparison between the interpreted paleo-drainage network and the modern drainage network, suggests that uplift in the Gombori range was sufficiently rapid such that river(s) could not maintain antecedent gorges like they currently do in the eastern KFTB (see Forte *et al.* 2010).

The lack of precise age control for the Alazani series sediments and that our one successful burial age date only provides constraint for the time by which a drainage reorganization had been completed results in uncertainty in terms of when deformation initiated in the western KFTB. However, if we assume that (1) the age of the base of the $Al_1$ strata is between 2.7-2.5 Ma (the maximum permissible age of the Akchagyl stage in this region), and (2) reflects deposition before significant development of the western KFTB and that the age of the $Al_3$ strata is ~1 Ma (from our burial age date of sample GOMSS03), and (3) deposition of $Al_3$ reflects a time by which the drainage reorganization had been completed, this brackets the initiation age of the western KFTB to between 2.7 and 1 Ma. Comparison of this range of possible initiation ages with those observed in the far eastern end of the KFTB, which based on new age constraints (e.g. Lazarev *et al.* 2019) likely initiated at ~2.2-2.0 Ma, suggests that if there was eastward along-strike propagation of the KFTB as suggested by Forte *et al.* (2010), it took no more than 0.5-1 Ma. Given the lingering uncertainty in the initiation age of the western KFTB

and the newly revised, older age of initiation in the eastern KFTB, it is equally viable that there was no significant propagation along-strike. This uncertainty highlights the need for additional work to establish the ages of the Alazani series stratigraphy in the western KFTB and identify additional areas where the timing of initiation of the KFTB can be assessed along strike.

**5.b. Implications for regional tectonics and seismic hazard**

Coarse spatial resolution GPS-derived crustal motion velocity data suggests an eastward horizontal velocity increase along-strike within the KFTB (see Reilinger *et al.* 2006). However, our tectonic geomorphologic analyses suggest that the rates of uplift along-strike within the Gombori range are not well-correlated with GPS horizontal velocities (with respect to Eurasia). In detail, our results indicate that the western Gombori range may be experiencing more rapid uplift, leading to its generally higher elevation, normalized channel steepness, and local relief. There could be several explanations for this apparent disconnect between an eastward increase in GPS velocity with an eastward decrease in local relief within the Gombori: 1) the along-strike decrease in relief reflects structural complexity with larger portions of the total convergence being taken up by additional structures to the south east of the Gombori, 2) an along-strike change in the ratio of shortening accommodated either currently or through time between the KFTB and the interior of the GC, 3) an along-strike change in structural geometry between steeper to shallower dipping structures from west to east within the KFTB that would result in an eastward decrease in the relationship between incremental total-shortening and vertical rock uplift, 4) a first order control from lithology such that once there is sufficient exhumation to expose older, more resistant units in the core of folds this lead to an increase in relief compared to adjacent areas which expose younger, less resistant units, even if those areas are experiencing greater rates of rock uplift, 5) the modern GPS velocity field is not representative of the long-term, i.e. several million year,

rate of convergence in the region, a suggestion which has been made more broadly for the GC as a whole (Forte *et al.* 2016), or 6) the Gombori itself reflects an eastward propagating set of structures.

At present, we do not have the data to uniquely select between these hypotheses. Option 1 would be consistent with coarse resolution syntheses of structures and estimation of activity of those structures presented in Forte *et al.* (2010), but without quantitative assessments of the amounts of total shortening accommodated by structures southeast of the Gombori (or in the Gombori itself), this is hard to validate. Similarly, option 2 would be consistent with an eastward along-strike decrease in range front sinuosity for the frontal GC, used as a proxy for time since the GC range front fault was active at the surface, as noted by Forte et al, 2010, but generally not consistent with other observations within the Eastern GC of no clear differences along-strike in terms of the tectonic geomorphology of this portion of the range (e.g. Forte *et al.* 2014, Forte *et al.* 2015). Option 3 is not broadly consistent with the observed bedding orientations within the Gombori as, at least within the Alazani Series, there does not appear to be any clear change in the orientation of units along-strike, e.g. $Al_1$ facies sediments uniformly dip $50^0$-$60^0$ along the exposed portion of the Alazani series. For option 4, our analyses of the topography did not indicate that lithology exerts a strong control, but importantly our analyzes did not extend beyond the Gombori range. Fully evaluating option 5 or 6 requires detailed estimations of total-shortening and timing of initiation along-strike within the KFTB and the Gombori, however it is worth noting that as discussed in the previous section, our results along with updated chronology for stage boundaries, have narrowed the range of time over which the KFTB would need to propagate eastward along-strike, leaving open the possibility that a fundamental disconnect between GPS rates and long-term geologic rates is viable. Ultimately, this work further highlights the necessity of detailed estimates of amounts of total shortening and ages of deformation initiation throughout the KFTB.

Previous work from the Eastern (Forte *et al.* 2013) and Central (Alania *et al.* 2017) KFTB concluded that Kura foreland is an active fold-thrust belt. Our study revealed that the Western portion of this belt has

experienced large scale tectonic movements and drainage reorganization that are still in progress. GPS data from the western neighboring region showed that Tbilisi and the northern boundary of the Lesser Caucasus is a zone of active convergence (Sokhadze *et al.* 2018) and the sparse GPS network from the Gombori range and GC indicated horizontal velocity gradient between the Gombori and the GC (after Akhalaia, Onur *et al.* 2019). All these data, from different sources lead us to assume that the Western KFTB is actively deforming and it should be considered during seismic hazard assessment of the region.



## 6. Conclusions

Our synthesis of the tectonic geomorphology, absolute age dating of syn-tectonic Plio-Pleistocene sediments within the Kura Fold-Thrust Belt, and paleocurrent analyses within those same sediments shed new light on both the history and current state of active deformation within the Western Kura Fold-Thrust Belt. The results reveal a Plio-Pleistocene drainage reorganization event within the northwestern corner of the southeastern foreland of the Greater Caucasus Mountains, which appears linked to initiation and development of the Kura Fold-Thrust Belt. If the timing of this drainage reorganization event, constrained to have occurred between ~2.7-1 Ma, is representative of initiation of this western-most segment of the KFTB, then this is still consistent with the idea of an eastward propagating KFTB as originally proposed by Forte *et al.* (2010), but implies that along-strike propagation of the fold-thrust belt along its ~300 km length took no more than ~1 million years and leaves open the possibility of no significant along-strike diachroneity in fold-thrust belt initiation. Quantitative tectonic geomorphic analyses of the Gombori range indicate that the Western Kura Fold-Thrust belt is still a zone of active deformation, especially its NW segment. This is consistent with recently

published, preliminary GPS velocity data (after Akhalaia, Onur *et. al,* 2019) suggestive of a velocity gradient between the Western Kura Fold-Thrust Belt and Greater Caucasus Mountains. In aggregate, our results highlight that potential seismic activity within the Gombori Range and northwestern Kura Fold-Thrust Belt should be considered when assessing seismic hazard for the densely populated (~1.2 million people) Georgian capital city of Tbilisi, which lies less than 50 km away from our study sites.

*Supplementary Material is available on the Cambridge Journals Online website*

**Acknowledgments**

This work was supported by:

This research [#PhDF2016_208 and #IG 29/1/16] has been supported by Shota Rustaveli National Science Foundation of Georgia (SRNSFG);

Louisiana State University;

United States National Science Foundation grant EAR-1450970 to Adam M. Forte and Kelin X. Whipple;

Institute of Earth Sciences and National Seismic Monitoring Centre, Ilia State University;

Arizona State University.

**Conflict of interest.** None

*Figure 1. Location and topography of KFTB*

Figure 2. Earthquake events of KFTB from Complete Catalogue of Instrumental Seismicity for Georgia (Onur *et al.* 2019), fault plane solution by (Tan & Taymaz, 2006)

Figure 3. Stratigraphy of the Gombori range compiled after (Buleishvili, 1974), (Zedginidze *et al.* 1971), (Kereselidze, 1950), (Sidorenko & Gamkrelidze, 1964), (Buachidze *et al.* 1950). Thicknesses are approximate and likely vary along-strike within the Gombori Range

Figure 4. Base of Al1 series from catchment 7, view to the NW showing steeply, NE dipping conglomeratic (a) and sandy loam (b) beds

Figure 5. NE dipping volcanic ash layer exposed in catchment 12, facies 2

Figure 6. TRMM 3B42 pixel extends (black) and catchments of the study area (red) and the identifying numbers for those catchments referenced in the text

Figure 7. Simplified lithology, sampling sites and paleocurrent directions

Figure 8. Topography and local relief maps of catchments (upper). Catchment averaged and stream $k_{sn}$ values (below). See text for details of these calculations

Figure 9. correlation matrix of different indices. Units: Local relief – meter; Mean elevation – meter; Mean slope – degree; K (Cretaceous rocks) – Percentage of catchment covered by these rocks; AkAp (Akchagyl-Apsheron) - Percentage of catchment covered by these rocks; TRMM - millimeter/annual mean

Figure 10. Swath profile of topography, $k_{sn}$ values (upper graph) and along swath geomorphologic indices and rainfall data

Figure 11. Erosion island plot for Gombori range samples. Variability in production rate scaling for the two samples, GOMSS01 and GOMSS03 are reflected in the pairs of points. Sample GOMSS01 plots in the forbidden zone and are thus interpretable. Sample GOMSS03 have mean ages of ~1 Ma regardless of exact scaling relationships used. The relatively high uncertainties on the ages reflect high native Al concentrations. Burial isochrons are reported in Ma and bounds for estimated paleo erosion rates in cm/ka. Plots produced using CosmoCalc (Vermeesch, 2007)

Figure 12. Fluvial system evolution diagram for the western KFTB. A) During the deposition of Alazani Suite1 ($Al_1$), rivers draining from the Greater Caucasus were still able to flow directly south across what is now the KFTB. B) Alazani Suite 2 ($Al_2$) represents deposition in a lacustrine setting, which could relate to damming of rivers by growth of the KFTB, or could be related to broader, basin wide changes in base-level. C) By the time of deposition of Alazani Suite 3 ($Al_3$), the river network in the northwestern KFTB had developed into something similar to the modern, with rivers draining northward out of the Gombori range and with a well-defined axial drainage occupying the Alazani basin

*Table 1. Burial age sampling site information*

| Sample name | Date of collection | Location | Elevation (m) | Facies |
|---|---|---|---|---|
| **GOMSS01** | 26-Apr-2017 | 41.80815, 45.34789 | 1831 | $Al_1$(?) |
| **GOMSS02** | 09-Mar-2017 | 41.92953, 45.40144 | 749 | $Al_3$ |
| **GOMSS03** | 09-Mar-2017 | 41.928925, 45.395784 | 768 | $Al_3$ |

Table 2. Von Mises distribution results for the paleocurrent measurements

| Catchment | Facies | Number of measurements | Max value (%) | Orientation (deg.) | Mean vector (deg.) |
|---|---|---|---|---|---|
| **7** | $Al_1$ | 36 | 56 | 221-240 | 225.4±3.6 |
| **7** | $Al_3$ | 52 | 17 | 61-80 | 142.4±20.4 |
| **11** | $Al_1$ | 93 | 63 | 201-220 | 214.7±2.2 |
| **11** | $Al_3$ | 73 | 18 | 101-120 | 67±25.8 |

**References**

Adamia, Sh, V. Alania, A. Chabukiani, G. Chichua, O. Enukidze, & N. Sadradze. 2010. "Evolution of the Late Cenozoic Basins of Georgia (SW Caucasus): A Review." *Geological Society Special Publication* 340: 239–59. https://doi.org/10.1144/SP340.11.

Adamia, Shota, Victor Alania, Aleksandre Chabukiani, Zurab Kutelia, & Nino Sadradze. 2011. "Great Caucasus ( Cavcasioni ): A Long-Lived North-Tethyan Back-Arc Basin" 20: 611–28. https://doi.org/10.3906/yer-1005-12.

Ahnert, Frank. 1970. "Functional Relationships between Denudation, Relief, and Uplift in Large, Mid-Latitude Drainage Basins." *American Journal of Science* 268: 243–63. https://doi.org/10.2475/ajs.268.3.243.

Alania, Victor, A. Chabukiani, R. Chagelishvili, Onice Enukidze, K. Gogrichiani, A. Razmadze, & Nino Tsereteli. 2017. "Growth Structures, Piggy-Back Basins and Growth Strata of the Georgian Part of the Kura Foreland Fold-Thrust Belt: Implications for Late Alpine Kinematic Evolution." *Geological Society, London, Special Publications* 428: 171–85. https://doi.org/10.1144/SP428.5.

Allmendinger, Richard W., Nestor Cardozo, & Donald M. Fisher. 2011. *Structural Geology Algorithms*. https://doi.org/10.1017/CBO9780511920202.

Avdeev, Boris, & Nathan A. Niemi. 2011. "Rapid Pliocene Exhumation of the Central Greater Caucasus Constrained by Low-Temperature Thermochronometry." *Tectonics*. https://doi.org/10.1029/2010TC002808.

Baak, Christiaan G.C. Van, Arjen Grothe, Keith Richards, Marius Stoica, Elmira Aliyeva, Gareth R. Davies, Klaudia F. Kuiper, & Wout Krijgsman. 2019a. "Flooding of the Caspian Sea at the

Intensification of Northern Hemisphere Glaciations." *Global and Planetary Change* 174: 153–63. https://doi.org/10.1016/j.gloplacha.2019.01.007.

Bookhagen, Bodo, & Douglas W. Burbank. 2006. "Topography, Relief, and TRMM-Derived Rainfall Variations along the Himalaya." *Geophysical Research Letters* 33 (8): 1–5. https://doi.org/10.1029/2006GL026037.

Bookhagen, Bodo, & Manfred R. Strecker. 2008. "Orographic Barriers, High-Resolution TRMM Rainfall, and Relief Variations along the Eastern Andes." *Geophysical Research Letters* 35 (6): 1–6. https://doi.org/10.1029/2007GL032011.

Bretis, Bernhard, Nikolaus Bartl, & Bernhard Grasemann. 2011. "Lateral Fold Growth and Linkage in the Zagros Fold and Thrust Belt (Kurdistan, NE Iraq)." *Basin Research* 23 (6): 615–30. https://doi.org/10.1111/j.1365-2117.2011.00506.x.

Buachidze, I, K Gigauri, I Zviadadze, & T Pkhakadze. 1950. "Groundwater Resourse Estimations of Alazani Artesian Basin (in Russian)." Tbilisi: Ministry of Geology of USSR.

Buachidze, I, T Pkhakadze, & Sh Tsitsilashvili. 1952. "Alazani Artesian Basin (In Russian)." Tbilisi.

Burbank, Douglas, Andrew Meigs, & Nicholas Brozović. 1996. "Interactions of Growing Folds and Coeval Depositional Systems." *Basin Research* 8 (3): 199–223. https://doi.org/10.1046/j.1365-2117.1996.00181.x.

Champel, Bénédicte. 2002. "Growth and Lateral Propagation of Fault-Related Folds in the Siwaliks of Western Nepal: Rates, Mechanisms, and Geomorphic Signature." *Journal of Geophysical Research* 107 (B6). https://doi.org/10.1029/2001jb000578.

Chkhikvadze, V, G Mchedlidze, N Burchak-Abramovich, O Bendukidze, D Burchak, Ts Gabelaia, N Amiranashvili, G Meladze, E Kharabadz, & N Chkareuli. 2000. “Review of the Localities of Tertiary Vertebrates of Georgia (In Russian).” In , 153–60. Tbilisi: A. Janelidze Geological Institute, Georgian Academy of Sciences.

Cowgill, Eric, Adam M. Forte, Nathan Niemi, Boris Avdeev, Alex Tye, Charles Trexler, Zurab Javakhishvili, Mikheil Elashvili, & Tea Godoladze. 2016. “Relict Basin Closure and Crustal Shortening Budgets during Continental Collision: An Example from Caucasus Sediment Provenance.” *Tectonics* 35 (12): 2918–47. https://doi.org/10.1002/2016TC004295.

Davis, Kenneth, Douglas W Burbank, Donald Fisher, Shamus Wallace, & David Nobes. 2005. “Thrust-Fault Growth and Segment Linkage in the Active Ostler Fault Zone , New Zealand.” *Journal of Structural Geology* 27: 1528–46. https://doi.org/10.1016/j.jsg.2005.04.011.

Delcaillau, B., B. Deffontaines, L. Floissac, J. Angelier, J. Deramond, P. Souquet, H. T. Chu, & J. F. Lee. 1998. “Morphotectonic Evidence from Lateral Propagation of an Active Frontal Fold; Pakuashan Anticline, Foothills of Taiwan.” *Geomorphology* 24 (4): 263–90. https://doi.org/10.1016/S0169-555X(98)00020-8.

Delcaillau, Bernard. 2001. “Geomorphic Response to Growing Fault-Related Folds: Example from the Foothills of Central Taiwan.” *Geodinamica Acta* 14 (5): 265–87. https://doi.org/10.1080/09853111.2001.11432447.

Delcaillau, Bernard, Jean Michel Carozza, & Edgard Laville. 2006. “Recent Fold Growth and Drainage Development: The Janauri and Chandigarh Anticlines in the Siwalik Foothills, Northwest India.” *Geomorphology* 76 (3–4): 241–56.

https://doi.org/10.1016/j.geomorph.2005.11.005.

Desilets, Darin, Marek Zreda, & T. Prabu. 2006. “Extended Scaling Factors for in Situ Cosmogenic Nuclides: New Measurements at Low Latitude.” *Earth and Planetary Science Letters* 246 (3–4): 265–76. https://doi.org/10.1016/j.epsl.2006.03.051.

Dibiase, Roman A, Kelin X Whipple, Arjun M Heimsath, & William B Ouimet. 2010. “Landscape Form and Millennial Erosion Rates in the San Gabriel Mountains , CA.” *Earth and Planetary Science Letters* 289 (1–2): 134–44. https://doi.org/10.1016/j.epsl.2009.10.036.

Ditchburn, & Whitehead. 1994. “The Separation of 10Be from Silicates.” *3rd Workshop of the South Pacific Environmental Radioactivity Association*.

Douglass, John, & Mark Schmeeckle. 2007. “Analogue Modeling of Transverse Drainage Mechanisms.” *Geomorphology* 84 (1–2): 22–43. https://doi.org/10.1016/j.geomorph.2006.06.004.

Flint, J. J. 1974. “Stream Gradient as a Function of Order, Magnitude, and Discharge.” *Water Resources Research* 10 (5): 969–73. https://doi.org/10.1029/WR010i005p00969.

Forte, A. M., E. Cowgill, T. Bernardin, O. Kreylos, & B. Hamann. 2010. “Late Cenozoic Deformation of the Kura Fold-Thrust Belt, Southern Greater Caucasus.” *Bulletin of the Geological Society of America* 122 (3–4): 465–86. https://doi.org/10.1130/B26464.1.

Forte, A. M., & Eric Cowgill. 2013. “Late Cenozoic Base-Level Variations of the Caspian Sea: A Review of Its History and Proposed Driving Mechanisms.” *Palaeogeography, Palaeoclimatology, Palaeoecology* 386: 392–407.

https://doi.org/10.1016/j.palaeo.2013.05.035.

Forte, A. M., Eric Cowgill, Ibrahim Murtuzayev, Talat Kangarli, & Marius Stoica. 2013. "Structural Geometries and Magnitude of Shortening in the Eastern Kura Fold-Thrust Belt, Azerbaijan: Implications for the Development of the Greater Caucasus Mountains." *Tectonics* 32 (3): 688–717. https://doi.org/10.1002/tect.20032.

Forte, A. M., Eric Cowgill, & Kelin X. Whipple. 2014. "Transition from a Singly Vergent to Doubly Vergent Wedge in a Young Orogen: The Greater Caucasus." *Tectonics* 33 (11): 2077–2101. https://doi.org/10.1002/2014TC003651.

Forte, A. M., Dawn Y. Sumner, Eric Cowgill, Marius Stoica, Ibrahim Murtuzayev, Talat Kangarli, Mikheil Elashvili, Tea Godoladze, & Zurab Javakhishvili. 2015. "Late Miocene to Pliocene Stratigraphy of the Kura Basin, a Subbasin of the South Caspian Basin: Implications for the Diachroneity of Stage Boundaries." *Basin Research* 27 (3): 247–71. https://doi.org/10.1111/bre.12069.

Forte, A. M., Kelin X. Whipple, & Eric Cowgill. 2015. "Drainage Network Reveals Patterns and History of Active Deformation in the Eastern Greater Caucasus." *Geosphere* 11 (5): 1343–64. https://doi.org/10.1130/GES01121.1.

Forte, A. M, & Kelin X Whipple. 2018. "Short Communication : The Topographic Analysis Kit (TAK) for TopoToolbox." *Earth Surface Dynamics*, no. July: 1–9. https://doi.org/10.5194/esurf-2018-57.

Forte, A. M, Kelin X Whipple, Bodo Bookhagen, & Matthew W Rossi. 2016. "Decoupling of

Modern Shortening Rates , Climate , and Topography in the Caucasus." *Earth and Planetary Science Letters* 449: 282–94. https://doi.org/10.1016/j.epsl.2016.06.013.

Gallen, Sean F., & Karl W. Wegmann. 2017. "River Profile Response to Normal Fault Growth and Linkage: An Example from the Hellenic Forearc of South-Central Crete, Greece." *Earth Surface Dynamics* 5 (1): 161–86. https://doi.org/10.5194/esurf-5-161-2017.

Gosse, & Philips. 2001. "Terrestrial in Situ Cosmogenic Nuclides:Theory and Application." *Quaternary Science Reviews* 20: 1475–1560.

Granger, Darryl E., James W.Kirchner, & Robert C. Finkel. 1997. "Quaternary Downcutting Rate of the New River, Virginia, Measured from 26Al and 10Be in Cave-Deposited Alluvium." *Geology* 25 (2): 107–10. https://doi.org/10.1130/0091-7613(1997)025<0107:QDROTN>2.3.CO;2.

Granger, Darryl E., & Paul F. Muzikar. 2001. "Dating Sediment Burial with in Situ-Produced Cosmogenic Nuclides: Theory, Techniques, and Limitations." *Earth and Planetary Science Letters* 188 (1–2): 269–81. https://doi.org/10.1016/S0012-821X(01)00309-0.

Granger, Darryl E. 2006. "A Review of Burial Dating Methods Using 26Al and 10Be." *Special Paper 415: In Situ-Produced Cosmogenic Nuclides and Quantification of Geological Processes* 2415 (01): 1–16. https://doi.org/10.1130/2006.2415(01).

Jackson, James, & Dan Mckenzie. 1988. "The Relationship between Plate Motions and Seismic Moment Tensors, and the Rates of Active Deformation in the Mediterranean and Middle East." *Geophysical Journal* 93: 45–73.

Jackson, J. 1992. “Partitioning of Strike-Slip and Convergent Motion between Eurasia and Arabia in Eastern Turkey and the Caucasus.” *Journal of Geophysical Research* 97 (B9): 12471–79. https://doi.org/10.1016/j.cardfail.2009.04.002.

JAXA. 2017. “ALOS Global Digital Surface Model ( DSM ) ‘ ALOS World 3D-30m ’ ( AW3D30 ) Dataset Product Format Description Earth Observation Research Center ( EORC ), Japan Aerospace Exploration Agency ( JAXA ),” no. March: 11.

Jones, R. W., & M. D. Simmons. 1996. “A Review of the Stratigraphy of Eastern Paratethys (Oligocene-Holocene).” *Bulletins of Natural History Museum of London* 52 (27): 25–49.

Keller, E. A., Larry Gurrola, & T. E. Tierney. 1999. “Geomorphic Criteria to Determine Direction of Lateral Propagation of Reverse Faulting and Folding.” *Geology* 27 (6): 515–18. https://doi.org/10.1130/0091-7613(1999)027<0515:GCTDDO>2.3.CO;2.

Kereselidze, K. 1950. “Alazani Artesian Basin (In Russian).” Tbilisi.

Kirby, E, & Kelin X. Whipple. 2001. “Quantifying Rockuplift Rates via Stream pro Le Analysis.” *Geology* 29 (5): 415–18. https://doi.org/10.1130/0091-7613(2001)029<0415:QDRURV>2.0.CO;2.

Kirby, Eric, Kelin X. Whipple, Wenqing Tang, & Zhiliang Chen. 2003. “Distribution of Active Rock Uplift along the Eastern Margin of the Tibetan Plateau: Inferences from Bedrock Channel Longitudinal Profiles.” *Journal of Geophysical Research: Solid Earth* 108 (B4). https://doi.org/10.1029/2001JB000861.

Kirby, Eric, & Kelin X Whipple. 2012. “Expression of Active Tectonics in Erosional Landscapes.”

*Journal of Structural Geology* 44: 54–75. https://doi.org/10.1016/j.jsg.2012.07.009.

Kohl, C. P., & K. Nishiizumi. 1992. "Chemical Isolation of Quartz for Measurement of In-Situ - Produced Cosmogenic Nuclides." *Geochimica et Cosmochimica Acta* 56 (9): 3583–87. https://doi.org/10.1016/0016-7037(92)90401-4.

W. Krijgsman, A. Tesakov, T. Yanina, S. Lazarev, G. Danukalova, C.G.C. Van Baak, J. Agustí, M.C. Alçiçek, E. Aliyeva, D. Bista, A. Bruch, Y. Büyükmeriç, M. Bukhsianidze, R. Flecker, P. Frolov, T.M. Hoyle, E.L. Jorissen, U. Kirscher, S.A. Koriche, S.B. Kroonenberg, D. Lordkipanidze, O. Oms, L. Rausch, J. Singarayer, M. Stoica, S. van de Velde, V.V. Titov, & F.P. Wesselingh. 2018. "Quaternary Time Scales for the Pontocaspian Domain: Interbasinal Connectivity and Faunal Evolution." *Earth-Science Reviews* 188: 1–40. https://doi.org/10.1016/j.earscirev.2018.10.013.

Krijgsman. 2019. "Magneto-Biostratigraphic Age Constraints on the Palaeoenvironmental Evolution of the South Caspian Basin during the Early-Middle Pleistocene (Kura Basin, Azerbaijan)." *Quaternary Science Reviews* 222 (September): 105895. https://doi.org/10.1016/j.quascirev.2019.105895.

Lague, Dimitri. 2014. "The Stream Power River Incision Model: Evidence, Theory and Beyond." *Earth Surface Processes and Landforms* 39 (1): 38–61. https://doi.org/10.1002/esp.3462.

Lawton, Timothy F, Steven E Boyer, & James G Schmitt. 1994. "And Conglomerate Distribution , Cordilleran Fold." *Geology* 22: 339–42.

Lazarev, Sergei, Elisabeth L. Jorissen, Sabrina van de Velde, Lea Rausch, Marius Stoica, Frank P.

Wesselingh, Christiaan G.C. Van Baak, Tamara A. Yanina, Elmira Aliyeva, a Wout

Merritts, Dorothy J, Kirk R Vincent, $ Ellen E Wohl. 1994. “Long River Profiles, Tectonism, and Eustasy: A Guide to Interpreting Fluvial Terraces.” *Journal of Geophysical Research* 99: 14031–50.

Miao, Xiaodong, Huayu Lu, Zhen Li, & Guangchao Cao. 2008. “Paleocurrent and Fabric Analyses of the Imbricated Fluvial Gravel Deposits in Huangshui Valley, the Northeastern Tibetan Plateau, China.” *Geomorphology* 99 (1–4): 433–42. https://doi.org/10.1016/j.geomorph.2007.12.005.

Mifsud, Charles, Toshiyuki Fujioka, & David Fink. 2013. “Extraction and Purification of Quartz in Rock Using Hot Phosphoric Acid for in Situ Cosmogenic Exposure Dating.” *Nuclear Instruments and Methods in Physics Research, Section B: Beam Interactions with Materials and Atoms* 294: 203–7. https://doi.org/10.1016/j.nimb.2012.08.037.

Mitchell, Nate A., & Brian J. Yanites. 2019. “Spatially Variable Increase in Rock Uplift in the Northern U.S. Cordillera Recorded in the Distribution of River Knickpoints and Incision Depths.” *Journal of Geophysical Research: Earth Surface* 124 (5): 1238–60. https://doi.org/10.1029/2018JF004880.

Montgomery, David R., & Mark T. Brandon. 2002. “Topographic Controls on Erosion Rates in Tectonically Active Mountain Ranges.” *Earth and Planetary Science Letters* 201 (3–4): 481–89. https://doi.org/10.1016/S0012-821X(02)00725-2.

Mosar, Jon, Talat Kangarli, Martin Bochud, Ulrich A. Glasmacher, Annick Rast, Marie-Francoise

Brunet, & Marc Sosson. 2010. “Cenozoic-Recent Tectonics and Uplift in the Greater Caucasus: A Perspective from Azerbaijan.” *Geological Society, London, Special Publications* 340 (1): 261–80. https://doi.org/10.1144/SP340.12.

Nichols, Gary. 2009. *Sedimentology and Stratigraphy*. *2nd Edition*. John Wiley & Sons Ltd,.

Onur, T, Gok, R, Godoladze, T, Gunia, I, Boichenko, G, Buzaladze, A, Tumanova, N, Dzmanashvili, M, Sukhishvili, L, Javakishvili, Z, Cowgill, E, Bondar, I, & Yetirmishli, G. 2019. “PROBABILISTIC SEISMIC HAZARD ASSESSMENT FOR GEORGIA.” *Lawrence Livermore National Lab. (LLNL), Livermore, CA (United States)*. https://doi.org/10.2172/1511856.

Reilinger, Robert, McClusky, Simon Vernant, Philippe Lawrence, Shawn Ergintav, Semih Cakmak, Rahsan Ozener, Haluk Kadirov, Fakhraddin Guliev, Ibrahim Stepanyan, Ruben Nadariya, Merab Hahubia, Galaktion Mahmoud, Salah Sakr, K. ArRajehi, Abdullah Paradissis, Demitris Al-Aydrus, A. Prilepin, Mikhail Guseva, Tamara Evren, Emre Dmitrotsa, Andriy Filikov, S. V. Gomez, Francisco Al-Ghazzi & Riad Karam, Gebran. 2006. “GPS Constraints on Continental Deformation in the Africa-Arabia-Eurasia Continental Collision Zone and Implications for the Dynamics of Plate Interactions.” *Journal of Geophysical Research: Solid Earth* 111 (5): 1–26. https://doi.org/10.1029/2005JB004051.

Rossi, Matthew W., Mark C. Quigley, John M. Fletcher, Kelin X. Whipple, J. Jesús Díaz-Torres, Christian Seiler, L. Keith Fifield, & Arjun M. Heimsath. 2017. “Along-Strike Variation in Catchment Morphology and Cosmogenic Denudation Rates Reveal the Pattern and History of Footwall Uplift, Main Gulf Escarpment, Baja California.” *Bulletin of the Geological Society of America* 129 (7–8): 837–54. https://doi.org/10.1130/B31373.1.

Schwanghart, W., & D. Scherler. 2014. “Short Communication: TopoToolbox 2 - MATLAB-Based Software for Topographic Analysis and Modeling in Earth Surface Sciences.” *Earth Surface Dynamics* 2 (1): 1–7. https://doi.org/10.5194/esurf-2-1-2014.

Sidorenko, A, & P Gamkrelidze, eds. 1964. “Geology of USSR.” In *SSSR Geology (In Russian)*, 1–648. Moscow.

Snyder, Noah P, Kelin X. Whipple, Gregory E Tucker, Dorothy J Merritts, & Marshall College. 2000. “Stream Profiles in the Mendocino Triple Junction Region , Northern California.” *Geological Society of America Bulletin* 112 (8): 1250–63. https://doi.org/10.1130/0016-7606(2000)112<1250:lrttfd>2.3.co;2.

Sokhadze, G., M. Floyd, T. Godoladze, R. King, E. S. Cowgill, Z. Javakhishvili, G. Hahubia, & R. Reilinger. 2018. “Active Convergence between the Lesser and Greater Caucasus in Georgia: Constraints on the Tectonic Evolution of the Lesser–Greater Caucasus Continental Collision.” *Earth and Planetary Science Letters* 481: 154–61. https://doi.org/10.1016/j.epsl.2017.10.007.

Tadono, T., H. Nagai, H. Ishida, F. Oda, S. Naito, K. Minakawa, & H. Iwamoto. 2016. “Generation of the 30 M-MESH Global Digital Surface Model by Alos Prism.” *International Archives of the Photogrammetry, Remote Sensing and Spatial Information Sciences - ISPRS Archives* 41 (July): 157–62. https://doi.org/10.5194/isprsarchives-XLI-B4-157-2016.

Tan, O, & T Taymaz. 2006. “Active Tectonics of the Caucasus: Earthquake Source Mechanisms and Rupture Histories Obtained from Inversion of Teleseismic Body Waveforms.” *Postcollisional Tectonics and Magmatism in the Mediterranean Region and Asia* 409 (25):

531-578\r631. https://doi.org/10.1130/2006.2409(25).

Vermeesch, Pieter. 2007. “CosmoCalc: An Excel Add-in for Cosmogenic Nuclide Calculations.” *Geochemistry, Geophysics, Geosystems* 8 (8): 1–14. https://doi.org/10.1029/2006GC001530.

Vincent, Stephen J., William Braham, Vladimir A. Lavrishchev, James R. Maynard, & Melise Harland. 2016. “The Formation and Inversion of the Western Greater Caucasus Basin and the Uplift of the Western Greater Caucasus: Implications for the Wider Black Sea Region.” *Tectonics* 35 (12): 2948–62. https://doi.org/10.1002/2016TC004204.

Whipple, Kelin X. 2004. “Bedrock Rivers and the Geomorphology of Active Orogens.” *Annual Review of Earth and Planetary Sciences* 32 (1): 151–85. https://doi.org/10.1146/annurev.earth.32.101802.120356.

Whipple, Kelin X. 2009. “The Influence of Climate on the Tectonic Evolution of Mountain Belts.” *Nature Geoscience* 2 (2): 97–104. https://doi.org/10.1038/ngeo413.

Whittaker, Alexander C. 2012. “How Do Landscapes Record Tectonics and Climate?” *Lithosphere* 4 (2): 160–64. https://doi.org/10.1130/RF.L003.1.

Whittaker, Alexander C., & Sarah J. Boulton. 2012. “Tectonic and Climatic Controls on Knickpoint Retreat Rates and Landscape Response Times.” *Journal of Geophysical Research: Earth Surface* 117 (2): 1–19. https://doi.org/10.1029/2011JF002157.

Wobus, C, K X Whipple, E Kirby, N Snyder, J Johnson, K Spyropolou, B Crosby, & D Sheehan. 2006. “Tectonics from Topography: Procedurses, Promise, and Pitfalls.” *Geological Society*

*of America Special Paper* 398 (04): 55–74. https://doi.org/10.1130/2006.2398(04).

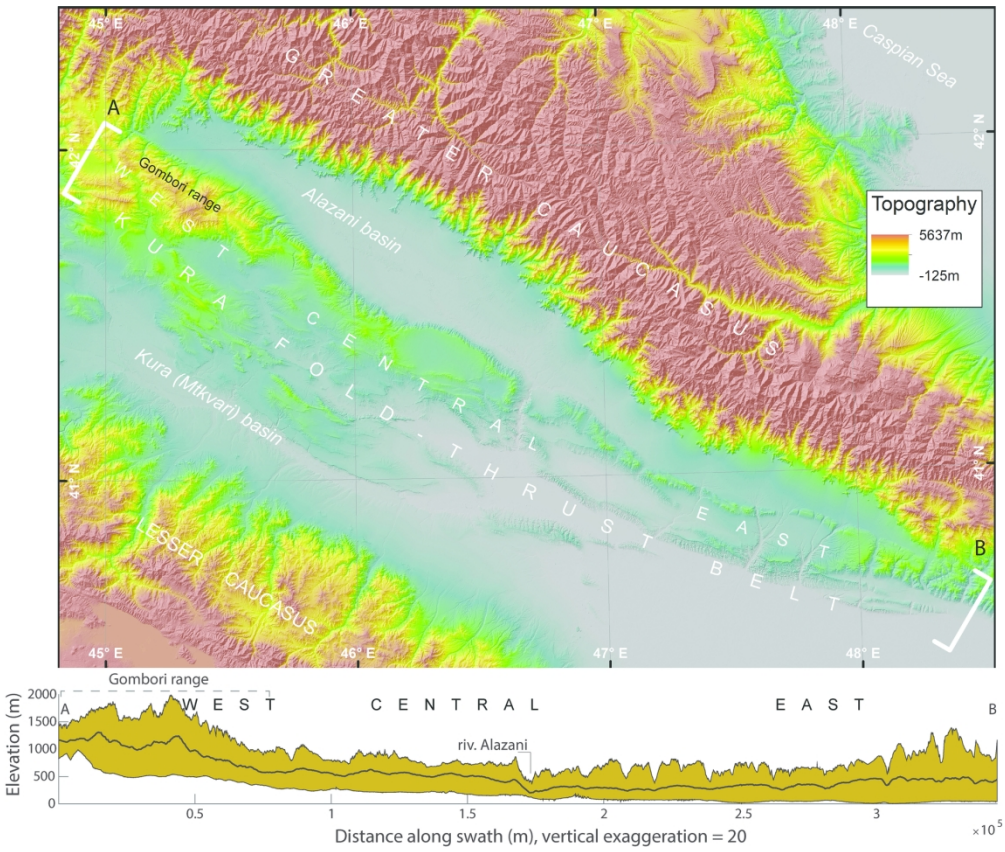


Figure 1. Location and topography of KFTB

168x141mm (300 x 300 DPI)

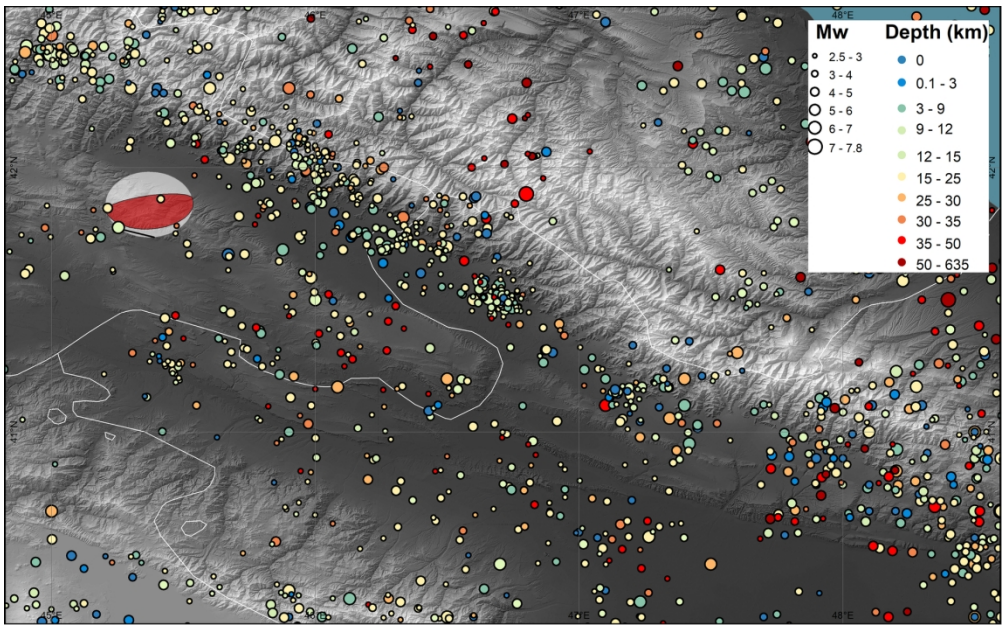


Figure 2. Earthquake events of KFTB from Complete Catalogue of Instrumental Seismicity for Georgia (Onur *et al.* 2019), fault plane solution by (Tan & Taymaz, 2006)

168x104mm (300 x 300 DPI)

| Period | Epoch | Stage | Suite | Thickness (m) | Lithology |
|---|---|---|---|---|---|
| Quaternary | | Upper Pleistocene - Holocene | | 50 | |
| | Pleistocene | Middle pleistocene | Alazani suite 3 | 200 | Cobble, conglomerate, loam and clay |
| | Pleistocene | Calabrian | Alazani suite 2 | 400 | Loam, clay, cobble and conglomerate |
| Neogene - Quaternary | Pliocene - Pleistocene | Gelasian- Middle Pleistocene | Akchagylian-Apsheronian, Alazani suite 1 | 1200 | Conglomerate, cobble, loam and clay |
| Neogene | Miocene | Tortonian-Messinian | Meotian-Pontian | 1500 | Upper: Conglomerates, Lower: sandstone and clay deposit |
| Paleogene | Eocene and Oligocene | Priabonian-Rupelian | Kint | 350+115 | Clay wih sandstone layers + arkosic and arkosic-greywacke sandstone and clay |
| Lower and Upper Cretaceous | Upper | Upper Turonian | Margalitis klde | 65 | Limestone, marl and clay |
| | Upper | Upper Cenomanian, Lower Turonian | Ananuri | 50 | Claystone and marl |
| | Upper | Cenomanian | Ukugmarti | 150 | Sandstone, limestone and claystone |
| | Lower | Albian | Navtiskhevi | 150 | Clay, marl, claystone and sandstone |
| | Lower | Aptian | Tempakhevi | 300 | Clay, claystone, sandstone, marl, limestone |

Figure 3. Stratigraphy of the Gombori range compiled after (Buleishvili, 1974), (Zedginidze *et al.* 1971), (Kereselidze, 1950), (Sidorenko & Gamkrelidze, 1964), (Buachidze *et al.* 1950). Thicknesses are approximate and likely vary along-strike within the Gombori Range

168x117mm (600 x 600 DPI)

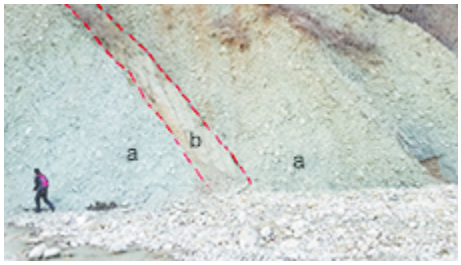


Figure 4. Base of $Al_1$ series from catchment 7, view to the NW showing steeply, NE dipping conglomeratic (a) and sandy loam (b) beds

80x45mm (72 x 72 DPI)

Figure 5. NE dipping volcanic ash layer exposed in catchment 12, facies 2

80x34mm (300 x 300 DPI)

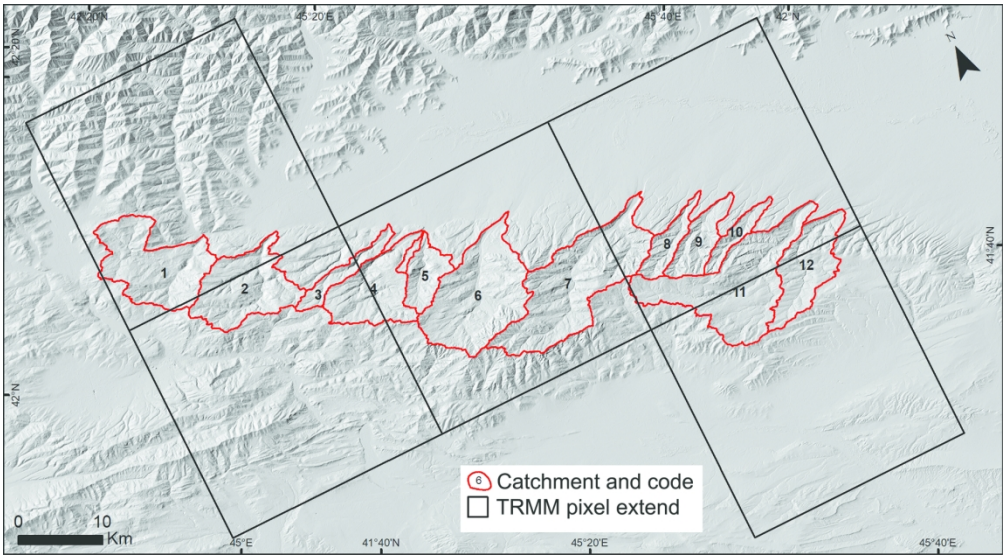


Figure 6. TRMM 3B42 pixel extends (black) and catchments of the study area (red) and the identifying numbers for those catchments referenced in the text

80x44mm (600 x 600 DPI)

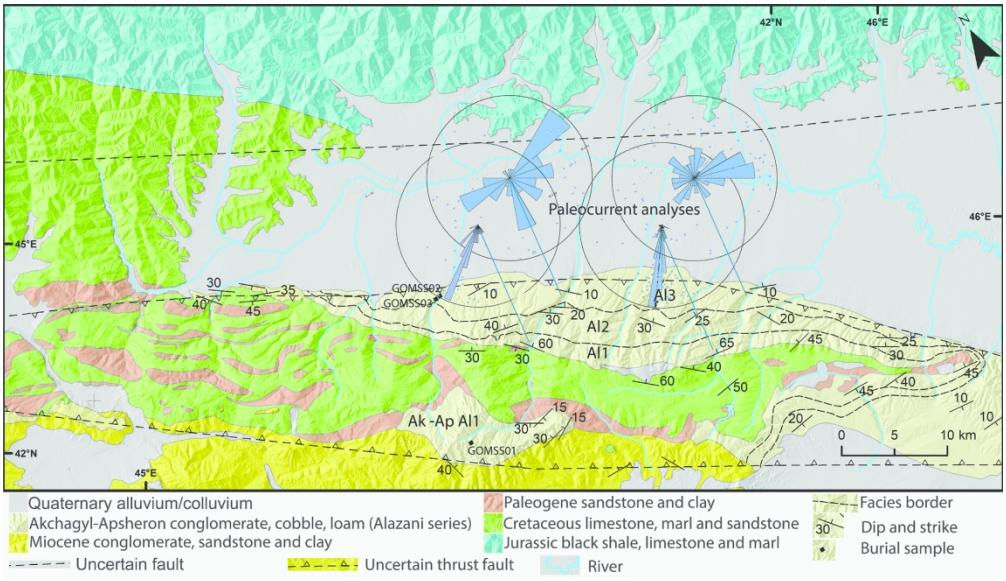


Figure 7. Simplified lithology, sampling sites and paleocurrent directions

168x97mm (300 x 300 DPI)

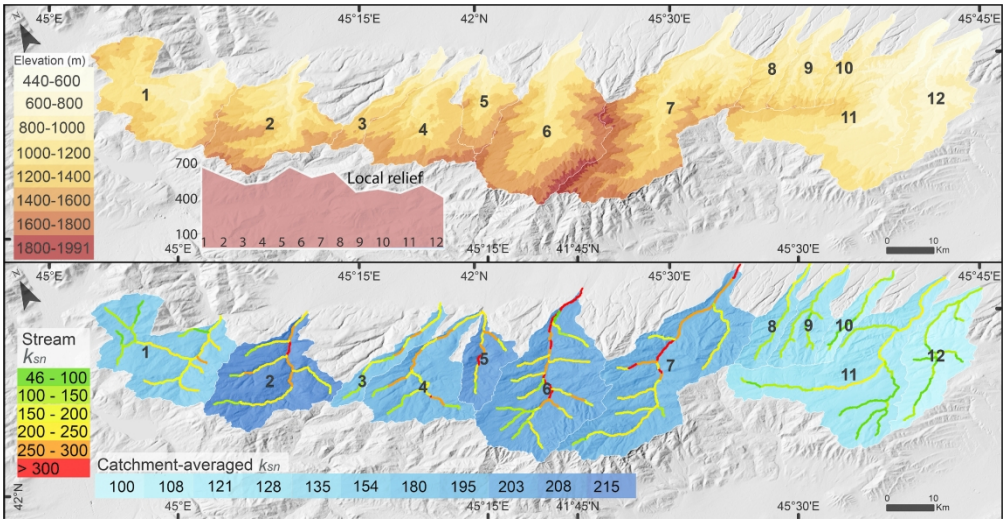


Figure 8. Topography and local relief maps of catchments (upper). Catchment averaged and stream $k_{sn}$ values (below). See text for details of these calculations

169x87mm (600 x 600 DPI)

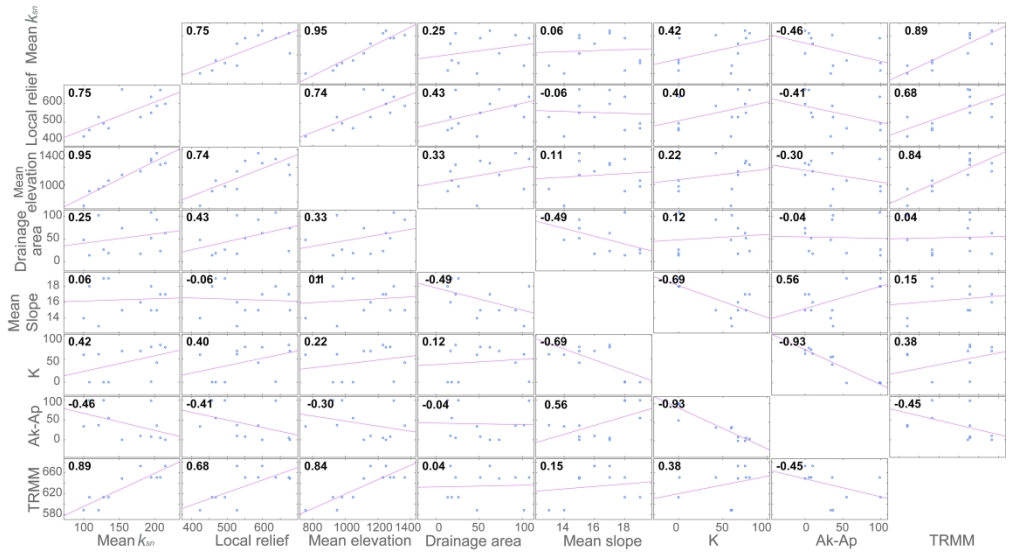


Figure 9. correlation matrix of different indices. Units: Local relief – meter; Mean elevation – meter; Mean slope – degree; K (Cretaceous rocks) – Percentage of catchment covered by these rocks; AkAp (Akchagyl-Apsheron) - Percentage of catchment covered by these rocks; TRMM - millimeter/annual mean

168x93mm (600 x 600 DPI)

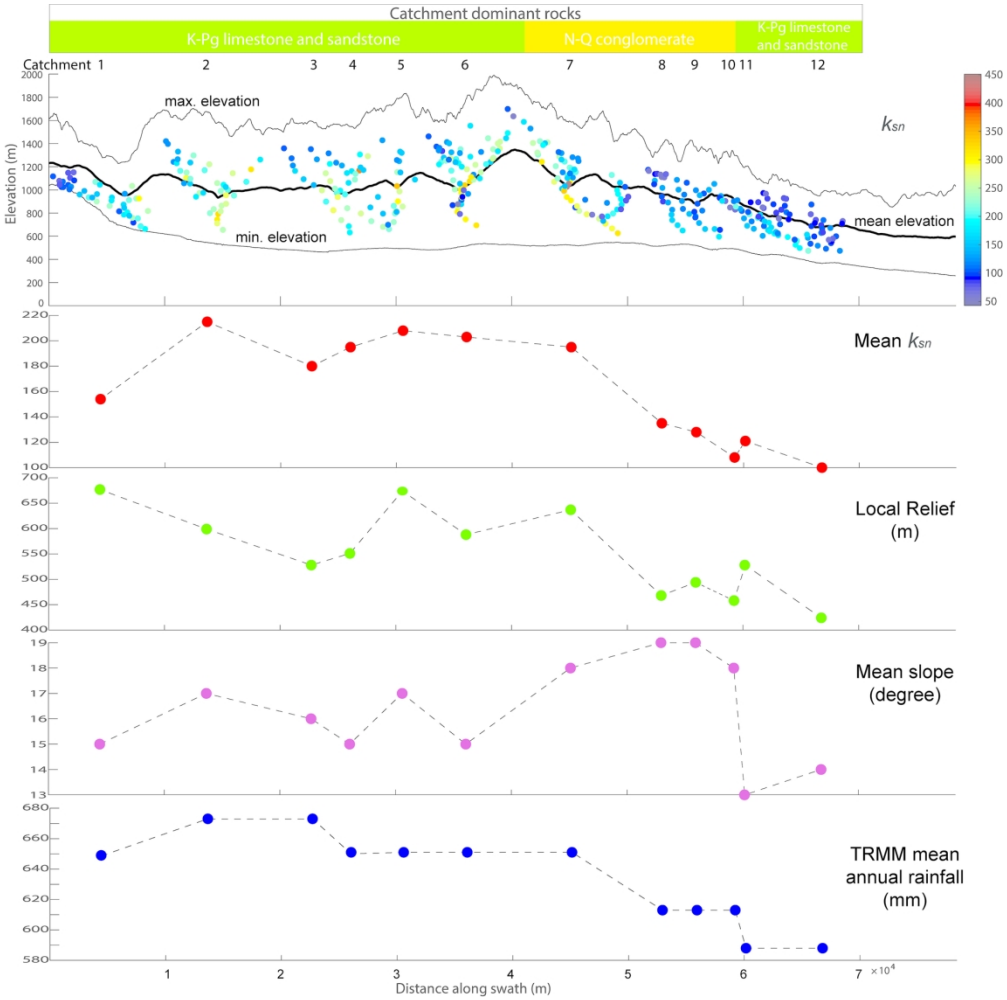


Figure 10. Swath profile of topography, $k_{sn}$ values (upper graph) and along swath geomorphologic indices and rainfall data

168x167mm (300 x 300 DPI)

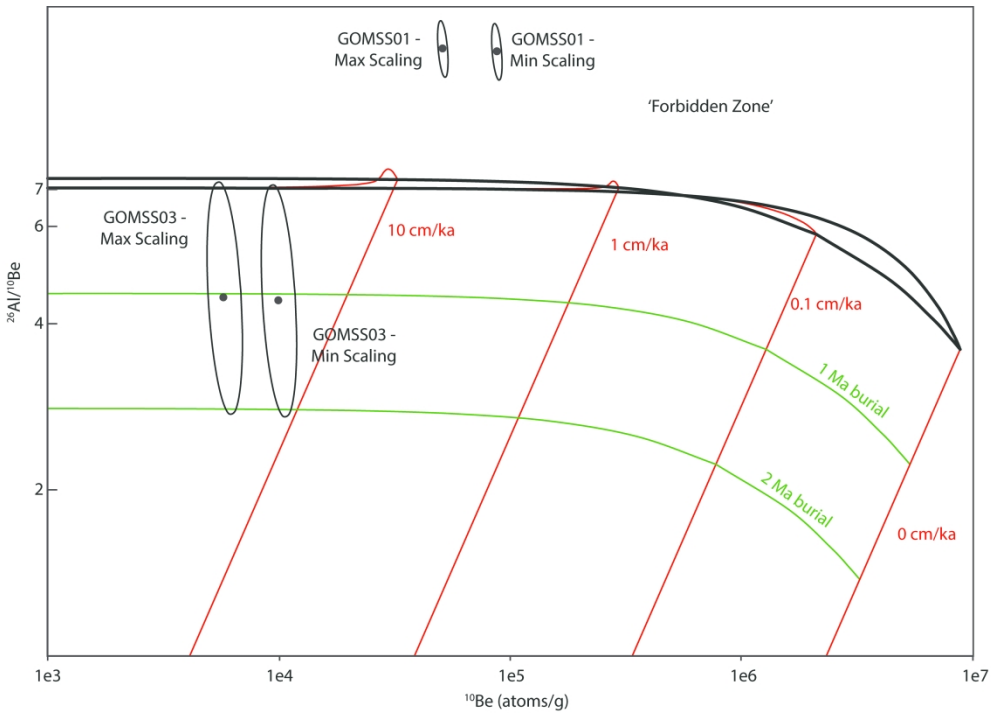


Figure 11. Erosion island plot for Gombori range samples. Variability in production rate scaling for the two samples, GOMSS01 and GOMSS03 are reflected in the pairs of points. Sample GOMSS01 plots in the forbidden zone and are thus interpretable. Sample GOMSS03 have mean ages of ~1 Ma regardless of exact scaling relationships used. The relatively high uncertainties on the ages reflect high native Al concentrations. Burial isochrons are reported in Ma and bounds for estimated paleo erosion rates in cm/ka. Plots produced using CosmoCalc (Vermeesch, 2007)

168x119mm (600 x 600 DPI)

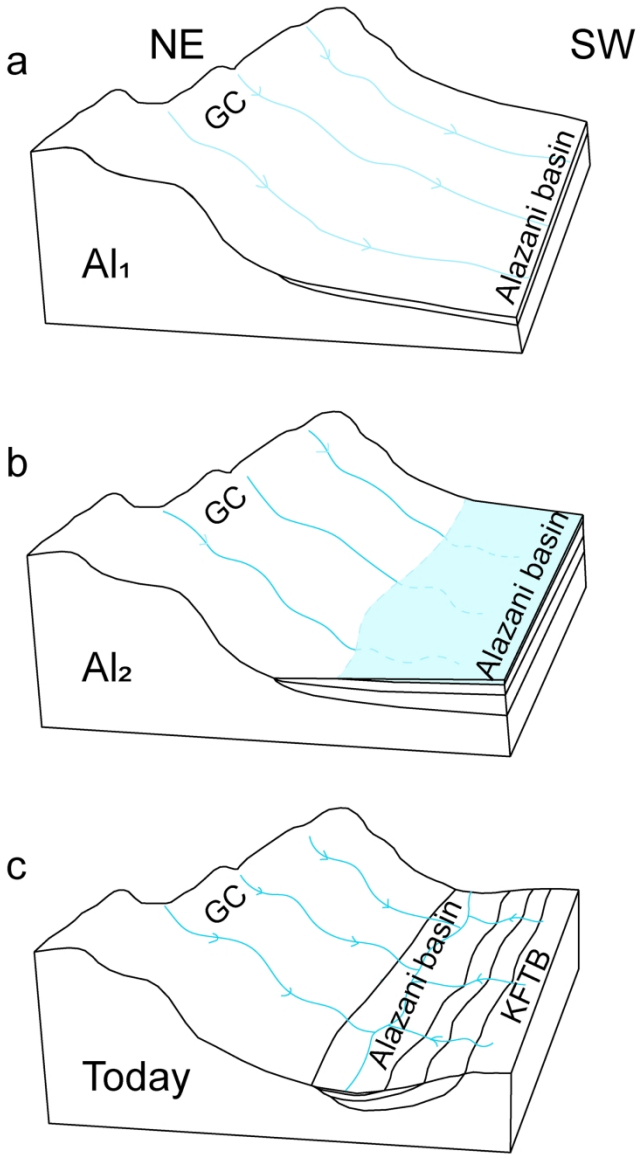


Figure 12. Fluvial system evolution diagram for the western KFTB. A) During the deposition of Alazani Suite1 (Al1), rivers draining from the Greater Caucasus were still able to flow directly south across what is now the KFTB. B) Alazani Suite 2 (Al2) represents deposition in a lacustrine setting, which could relate to damming of rivers by growth of the KFTB, or could be related to broader, basin wide changes in base-level. C) By the time of deposition of Alazani Suite 3 (Al3), the river network in the northwestern KFTB had developed into something similar to the modern, with rivers draining northward out of the Gombori range and with a well-defined axial drainage occupying the Alazani basin

80x135mm (600 x 600 DPI)

Geological Magazine

# Active deformation and Plio-Pleistocene fluvial reorganization of the western Kura Fold-Thrust Belt, Georgia: implications for the evolution of the Greater Caucasus mountains and seismic hazard

Lasha Sukhishvili,

Adam M. Forte,

Giorgi Merebashvili,

Joel Leonard,

Kelin X. Whipple,

Zurab Javakhishvili,

Arjun Heimsath,

Tea Godoladze



Supplementary Material

Supplementary Table S1. Sample information for the three samples analyzed for burial-age dating

| Sample ID | Latitude (°N) | Longitude (°E) | Elevation (m) | Quartz mass (g) | Mass $^{9}$Be (g) | Mass $^{27}$Al (g) | $^{10}$Be/$^{9}$Be | ± | $^{26}$Al/$^{27}$Al | ± | $^{10}$Be (atoms/g) | ± | $^{26}$Al (atoms/g) | ± |
|---|---|---|---|---|---|---|---|---|---|---|---|---|---|---|
| GOMSS01 | 41.80815 | 45.34789 | 1831 | 49.7598 | 4.91E-04 | 4.8546E-02 | 2.8825E-13 | 6.7986E-15 | 1.0655E-13 | 5.5598E-15 | 1.88E+05 | 4.87E+03 | 2.32E+06 | 1.23E+05 |
| GOMSS02 | 41.92953 | 45.40144 | 749 | NA | NA | NA | NA | NA | NA | NA | NA | NA | NA | NA |
| GOMSS03 | 41.928925 | 45.395784 | 768 | 71.5252 | 4.88E-04 | 3.8899E-02 | 4.974E-14 | 4.0645E-15 | 7.5273E-15 | 1.7049E-15 | 2.12E+04 | 1.87E+03 | 9.14E+04 | 2.07E+04 |

*Supplementary Table S*1. Parameters used for the four different scaling schemes for calculating production rates of 26Al and 10Be for interpreting the burial age dating, see text for more detail

| Production site | Latitude | Longitude | Elevation | Rc (GV) | Atmospheric depth (g/cm$^2$) | Desilets et al 2006 $^{10}$Be scaling | Desilets et al 2006 $^{26}$Al scaling | Burial age (Ma) | 2.5 Percentile (Ma) | 97.5 Percentile (Ma) |
|---|---|---|---|---|---|---|---|---|---|---|
| 'Local' | 42.336 | 44.80 | 1858.2 | 4.74 | 825 | | | | | |
| | | | | | | 4.25 | 4.22 | 9.77E-01 | 4.84E-03 | 2.53E+00 |
| 'Avgari' | 42.1182 | 45.02 | 1226.2 | 4.81 | 892 | | | | | |
| | | | | | | 2.57 | 2.56 | 1.01E+00 | 7.93E-03 | 2.62E+00 |
| 'Iori' | 42.1942 | 45.4762 | 1226.2 | 4.79 | 903 | | | | | |
| | | | | | | 2.37 | 2.36 | 1.02E+00 | 1.53E-02 | 2.59E+00 |
| 'SE GC' | 41.8657 | 45.3458 | 1472.6 | 4.90 | 865 | | | | | |
| | | | | | | 3.12 | 3.10 | 9.76E-01 | 3.80E-03 | 2.23E+00 |